Electronic Supplementary Material (ESI) for Catalysis Science & Technology.
This journal is © The Royal Society of Chemistry 2019

Supporting Information - Stoichiometric Active Site Modification Observed by Alkali Ion Titrations of Sn-Beta

Samuel Gilbert Elliot*, Irene Tosi*, Sebastian Meier, Juan Salvador Martinez Espin and Esben Taarning

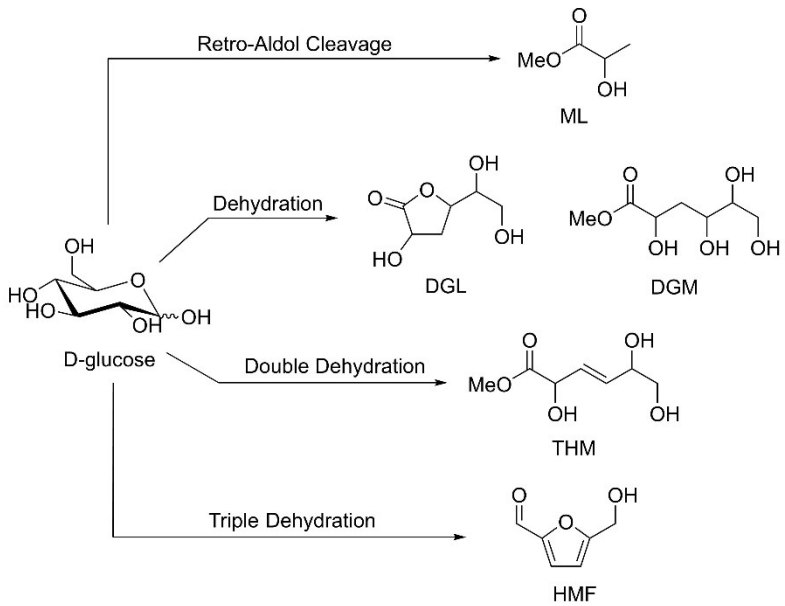

Scheme S1. Overview of major reaction products in this study. Detailed product overviews have previously been shown by Tolborg *et al.*[33, *main text*] ML = Methyl lactate. DGL = 3-deoxy-glucono-γ-lactone. DGM = 3-deoxy-gluconic acid methyl ester. THM = *trans*-2,5,6-trihydroxy-3-hexenoic acid methyl ester. HMF = 5-hydroxymethyl furfural.

Catalyst Characterization

Table S1. Physical properties of the catalysts used in the study measured using N_2-adsorption/desorption, XRD and NH_3-TPD.

Entry	Catalyst	Elemental Analysis	X-ray diffraction	N_2-adsorption				NH_3-TPD		
				S_{BET}	$S_{micropore}$[b]	V_{total}	$V_{micropore}$[b]	T_{max}[c]	Absorption	
		Si / Metal[a]	Primary Phase	m^2/g		mL/g		°C	µmol/g	mol/mol Sn[d]
1	Sn-Beta (PT, 25)	23	*BEA	617	415	1.01	0.166	257	172	0.26
2	Sn-Beta (PT, 50)	50	*BEA	638	433	1.01	0.174	263	123	0.38
3	Sn-Beta (PT, 100)	98	*BEA	645	439	1.07	0.177	255	67.0	0.40
4	Sn-Beta (PT, 150)	145	*BEA	657	454	1.10	0.183	248	40.4	0.36
5	Sn-Beta (PT, 200)	198	*BEA	657	444	1.06	0.179	252	31.5	0.38
6	Sn-Beta (PT, 400)	411	*BEA	661	425	1.12	0.163	258	15.7	0.39

[a] Based on elemental analysis of silicon and tin done by XRF. [b] Determined using the t-plot method. [c] Temperature at peak maximum. [d]

Ammonia-Temperature Programmed Desorption (NH_3-TPD)

The strength and the amount of acid sites in the catalysts were determined by Ammonia-Temperature Programmed Desorption using a Micromeritics AutoChem II 2920 Chemisorption Analyzer (Figure S1). Approximately 100 mg of sample was pre-treated in a quartz U-tube at 500 ˚C for 110 minutes under helium in order to eliminate residual water. Thereafter, it was cooled down to 150 ˚C and flushed with a flow of 1 vol.% ammonia in helium for 30 minutes. After the adsorption, the sample was treated in helium at 150˚C for 4 hours to remove the physisorbed NH_3. Finally, the ammonia desorption was measured with a Thermal Conductivity Detector (TCD) during increasing of the temperature from 150 ˚C to 500 ˚C using a 10 ˚C/min ramp rate.

Quantitative analysis of the NH_3-TPD measurements were performed by deconvolution of the spectra into two peaks (~256 °C and 402 °C) to remove the contribution observed in the dealuminated sample (Figure S1). Direct subtraction of the dealuminated sample was not deemed suitable, as the incorporation of tin modifies the quantity of available silanols, thus changing the baseline

contribution. The TCD detector was calibrated with the baseline and the ammonia signal prior to sample analysis, in order to directly produce quantitative measurements. Quantification of ammonia absorbed by tin sites was obtained by integration of the peak at 256 °C.

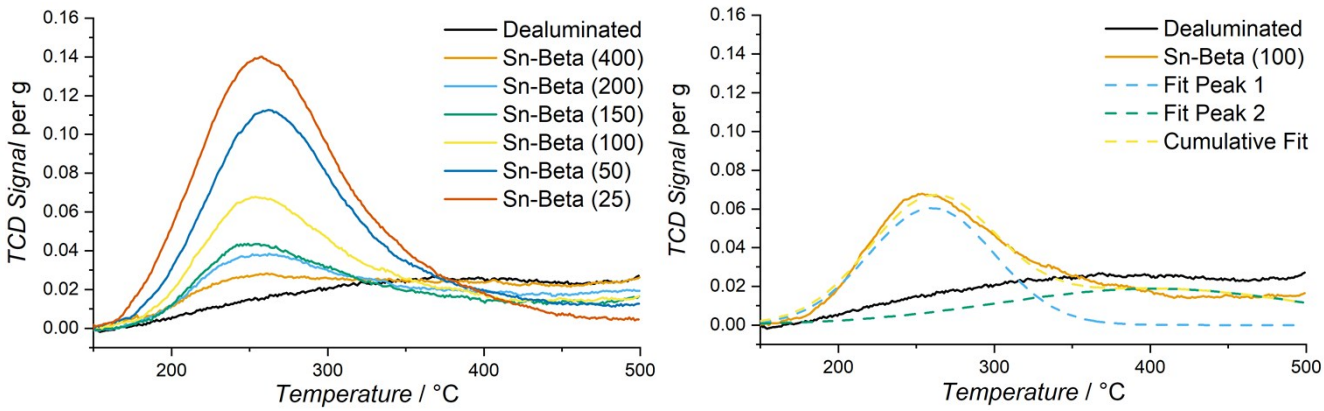

Figure S1. NH_3-TPD profiles of Sn-Beta zeolites with different Si/Sn content and the parental dealuminated beta zeolite (left), and an example of peak deconvolution of the Sn-Beta (PT, 100) catalyst (right).

X-Ray Powder Diffraction (XRD)

The XRD patterns of the synthesized catalysts showed the maintenance of the Beta structure of the zeolite after the treatment and the presence in traces of Sn oxides in the samples Sn-Beta (100) and Sn-Beta (50) and a significant amount in Sn-Beta (25) (FigureS2).

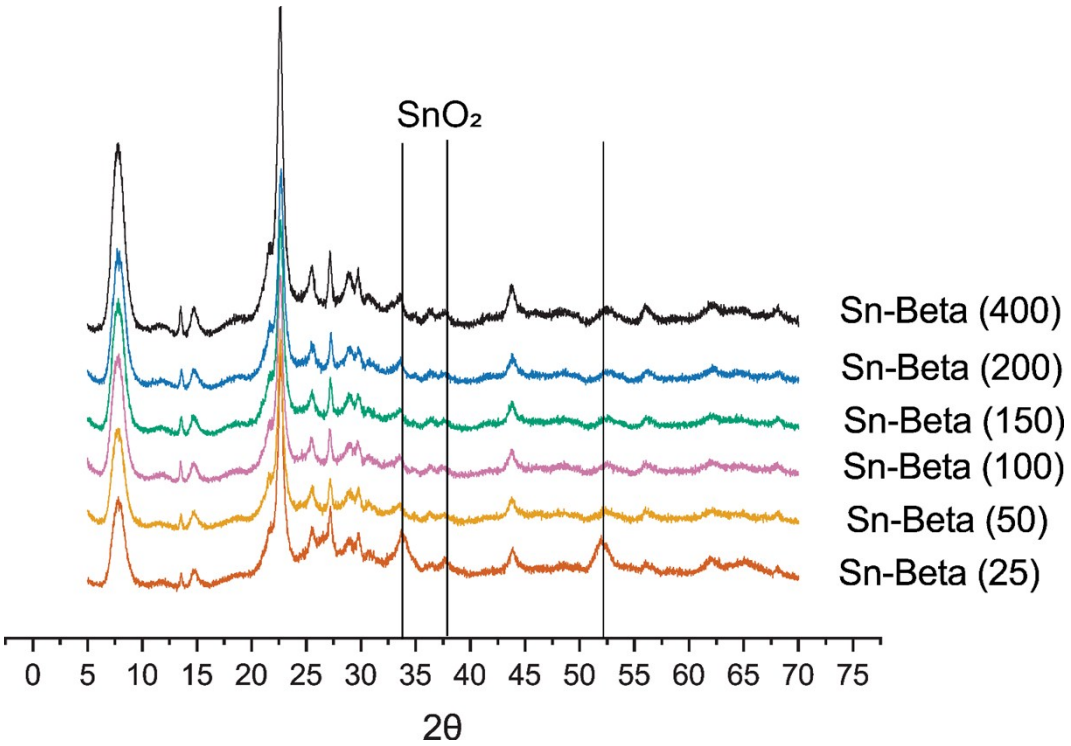

Figure S2. The powder XRD pattern of Sn-Beta zeolites.

Elemental analysis

The exact amount of Si, Sn and Al in the zeolites were determined by XRF analysis using a Supermini 200 instrument from Rigaku and dissolving the samples by making fused glass beads with lithium borate. In table S2 are reported the precise Si/Sn ratio for each catalyst.

All the samples were prepared by impregnation of the same parental dealuminated beta zeolite containing a Si/Al ratio of 12.5.

Please do not adjust margins

ICP analysis (Agilent 720 ICP) were used for the determination of the amount of traces of Na, K and Li and compare it to the impurity in a hydrothermally synthesized Sn-Beta (200) zeolite. All the samples contains traces of Na, K and Li in quantity < 40 wt ppm.

Scanning Electron Microscopy

The surface topology of the prepared catalysts was investigated by scanning electron microscopy using a FEI Quanta 200 ESEM FEG instrument. Figure S3 shows that the post-treated synthesis led to small-crystals materials (< 1 µm) and that samples containing different amount of Sn do not exhibit external differences.

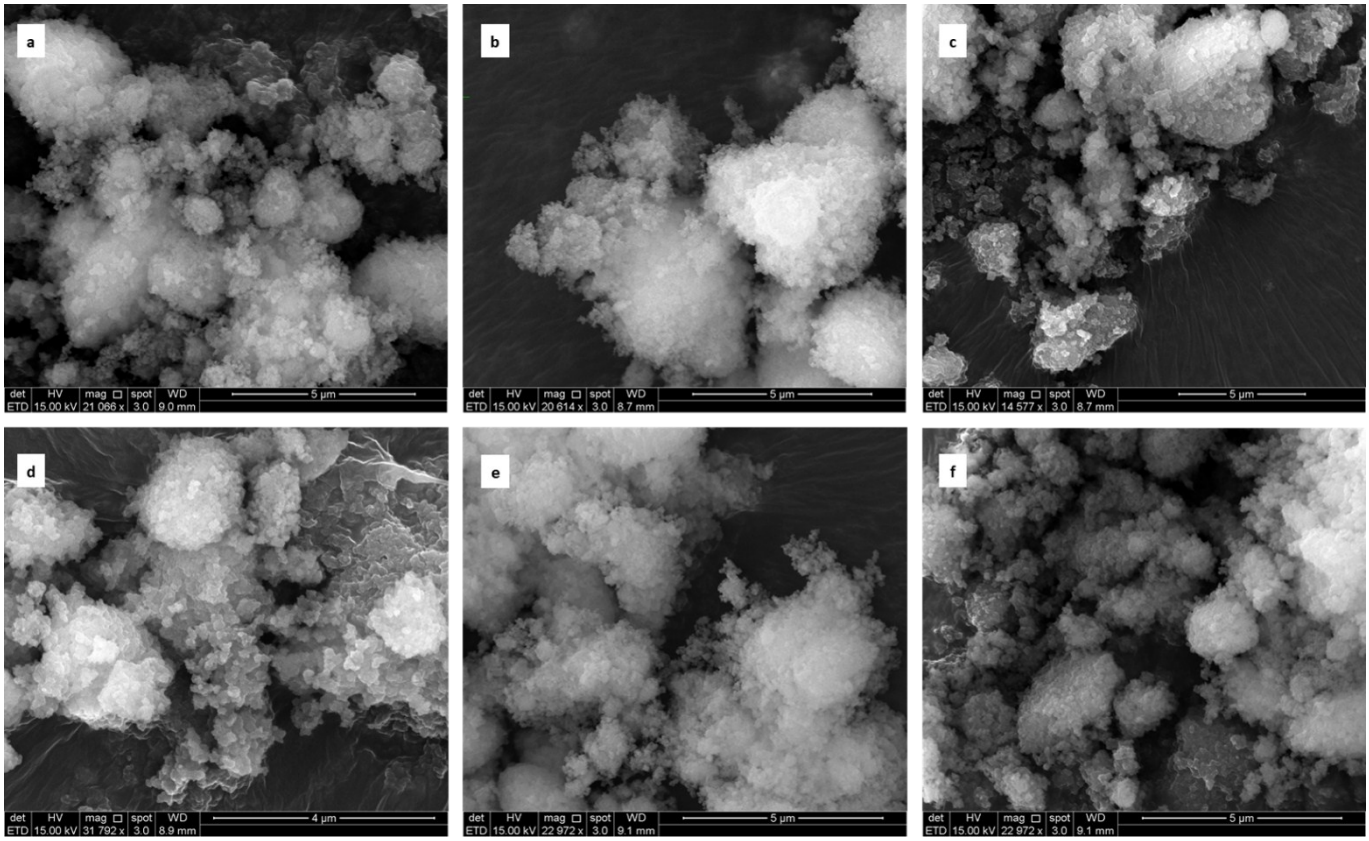

Figure S3. SEM images of post-treated zeolites, (a) parent dealuminated beta zeolite, (b) Sn-Beta (50), (c) Sn-Beta (100), (d) Sn-Beta (200), (e) Sn-Beta (400), (f) Sn-Beta (25)

Please do not adjust margins

Please do not adjust margins

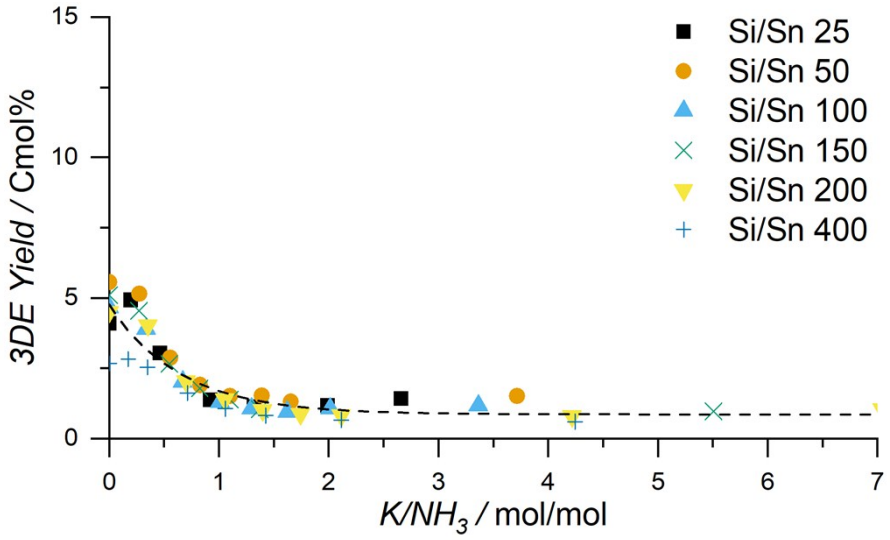

Figure S4. Effect of addition of potassium carbonate on the yield of the major single dehydration products, the 3-deoxy esters (3DE) 3-deoxyglucono-γ-lactone (DGL) and 3-deoxy-gluconic acid methyl ester (DGM), in the catalytic conversion of glucose by Sn-Beta (post-treatment synthesised) containing different amounts of Sn. The results are displayed with regard to the K/NH_3 ratio determined by NH_3-TPD and the curve is a guide to the eye. Reaction conditions: 360 mg D-Glucose, 90 mg Sn-Beta (post-treated), 55 mg DMSO (internal standard) and 5 mL potassium carbonate in methanol, reacted for 4 hours at 160 °C.

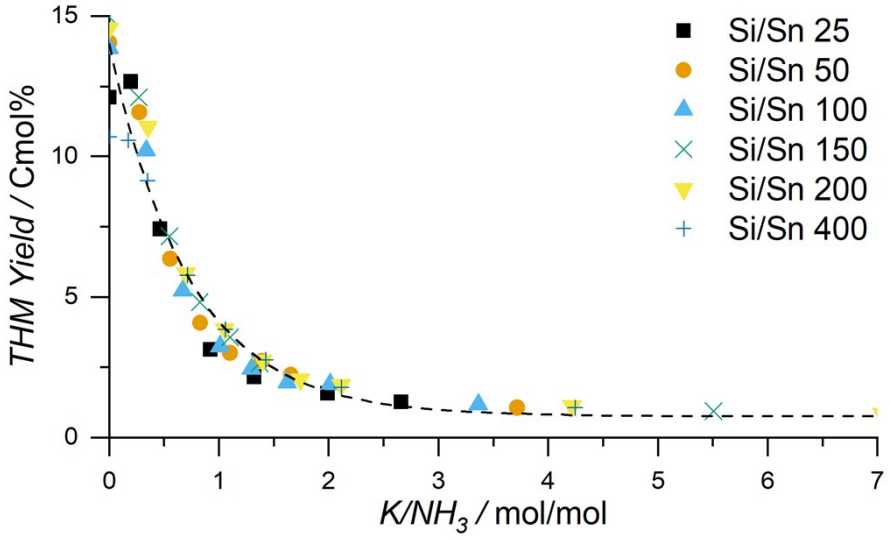

Figure S5. Effect of addition of potassium carbonate on the yield of the major double dehydration product *trans*-2,5,6-trihydroxy-3-hexenoic acid methyl ester (THM), in the catalytic conversion of glucose by Sn-Beta (post-treatment synthesised) containing different amounts of Sn. The results are displayed with regard to the K/NH_3 ratio determined by NH_3-TPD and the curve is a guide to the eye. Reaction conditions: 360 mg D-Glucose, 90 mg Sn-Beta (post-treated), 55 mg DMSO (internal standard) and 5 mL potassium carbonate in methanol, reacted for 4 hours at 160 °C.

Please do not adjust margins

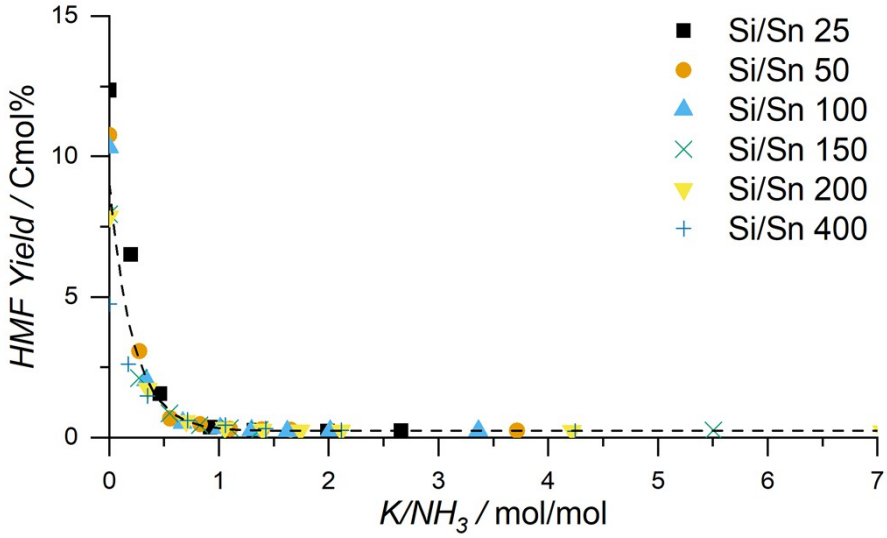

Figure S6. Effect of addition of potassium carbonate on the yield of the major double dehydration product 5-hydroxymethyl furfural (HMF), quantified in the dimethyl acetal form, in the catalytic conversion of glucose by Sn-Beta (post-treatment synthesised) containing different amounts of Sn. The results are displayed with regard to the K/NH_3 ratio determined by NH_3-TPD and the curve is a guide to the eye. Reaction conditions: 360 mg D-Glucose, 90 mg Sn-Beta (post-treated), 55 mg DMSO (internal standard) and 5 mL potassium carbonate in methanol, reacted for 4 hours at 160 °C.

Fitting of the Observed ML and THM yields to a Sequential Dissociation Model

The variation in observable ML yield as a function of potassium concentration was fitted to a sequential dissociation model (Figure S7). The yield was considered a linear combination for active sites with single and double exchange of a proton with a potassium ion, as two different regimes can be observed in the experimental curve (increasing and decreasing yield). The yield was described as

$$Yield = f_{(OH)_2} \cdot S_{(OH)_2 site} + f_{(OH)(OK)} \cdot S_{(OH)(OK)site} + f_{(OK)_2} \cdot S_{(OK)_2 site}$$

where f denotes the population (fraction) of the active site in either the double protonated $f_{(OH)_2}$, single-exchanged ($f_{(OH)(OK)}$) or double-exchanged form $f_{(OK)_2}$. S denotes the selectivities of the three sites for forming methyl lactate. Hence, the observed yield is approximated as a linear combination of selectivities for the three different sites weighted by their relative population at varying potassium concentrations. Populations were described by equations that are equivalent to populations in the titration of diprotic acids at varying [H⁺]. Fractions are described by two dissociation constants (normalized to tin active sites) κ_1 and κ_2, which leads to the description of the ML yield as

$$Yield = \frac{\kappa_1\kappa_2}{[K^+]^2 + [K^+]\kappa_1 + \kappa_1\kappa_2} \cdot S_{(OH)_2 site} + \frac{[K^+]\kappa_1}{[K^+]^2 + [K^+]\kappa_1 + \kappa_1\kappa_2} \cdot S_{(OH)(OK)site} + \frac{[K^+]^2}{[K^+]^2 + [K^+]\kappa_1 + \kappa_1\kappa_2} \cdot S_{(OK)_2 site}$$

The fit thus has five free parameters in κ_1 and κ_2 and the selectivities of the three sites $S_{(OH)_2 site}$, $S_{(OH)(OK)site}$ and $S_{(OK)_2 site}$. Data were fitted in *OriginPro 2018b* with selectivities limited to values between 0 and 100%. Fitted values for κ_1 and κ_2 were subsequently used to describe the yield of THM in a three-parameter-fit of the selectivities for THM $S_{(OH)_2 site}$, $S_{(OH)(OK)site}$ and $S_{(OK)_2 site}$ (Figure S7). This fit indicated that the κ_1 and κ_2 values for alkali exchange onto the zeolite active site are suitable for describing the dependence of the THM yield on the potassium concentration. Only the un-titrated site showed significant selectivity for THM at $S_{(OH)_2 site} \approx 14\%$.

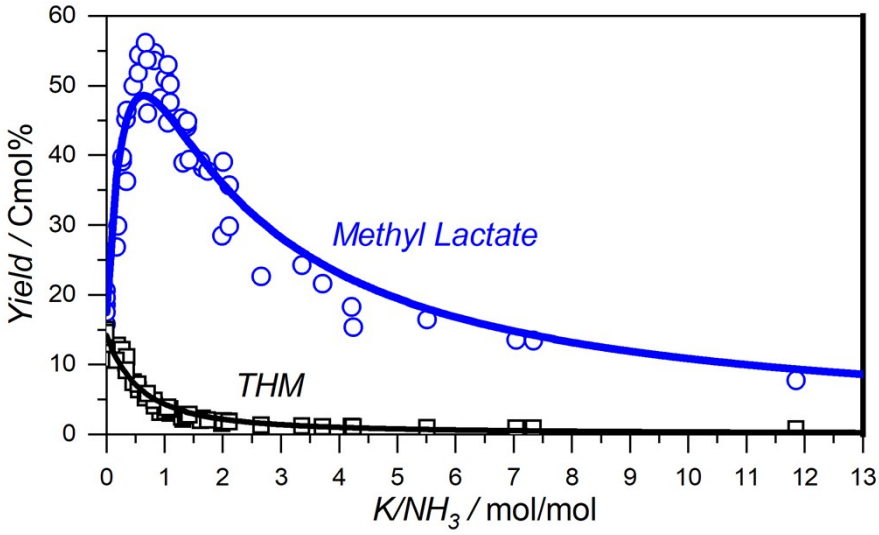

Figure S7. Fitting of all methyl lactate yields to a [K^+]-dependent double dissociation model (blue), demonstrating the optimal regimes for retro-aldol product formation, and fitting of all THM yields to a corresponding double dissociation model (black), to show the dehydration regime. Data points from all catalysts were employed, normalized to the number of Sn-active sites using NH_3-TPD. The fit of THM yields only varies the selectivity of the three different sites but employs dissociation constants obtained from the alkali-dependence of methyl lactate yields. The excellent agreement with experimental data indicates that identical structural changes lead to increasing methyl lactate yields and decreasing THM yields. The protonated active site has mediocre selectivity for THM (14% yield), which is abolished upon single (3% yield) and double exchange (0% yield) with potassium.

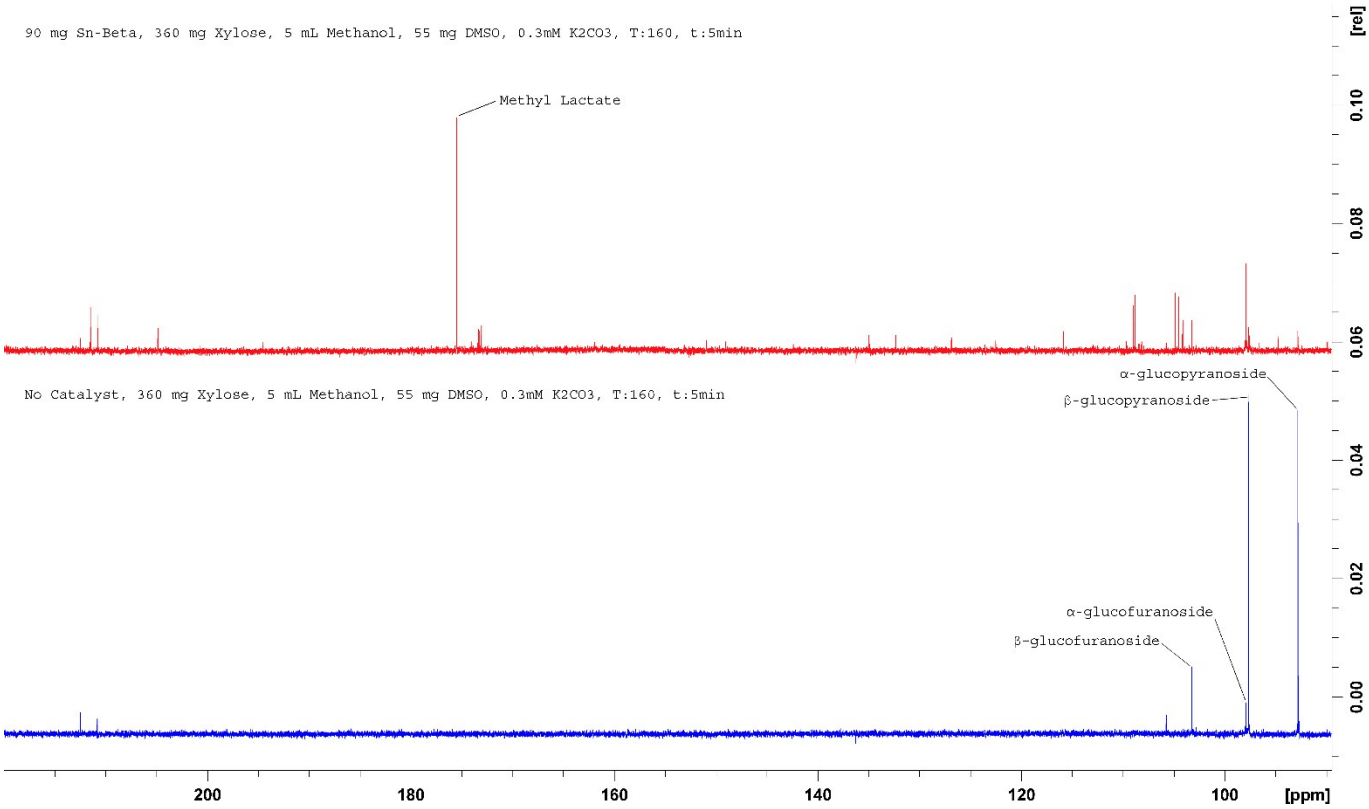

Figure S8. Comparison of ^{13}C NMR spectra of an experiment employing a Sn-Beta (200) catalyst (red) with a blank experiment containing no catalyst (blue). Both experiments contained 0.3 mM K_2CO_3 (close to the catalyst optimum for methyl lactate formation) and the lack of conversion in absence of the catalyst shows that no base catalyzed dehydration is taking place.